IEEE Access
Multidisciplinary | Rapid Review | Open Access Journal

Received July 1, 2020, accepted July 2, 2020, date of publication July 7, 2020, date of current version July 20, 2020.

Digital Object Identifier 10.1109/ACCESS.2020.3007597

Aggregator to Electric Vehicle LoRaWAN Based Communication Analysis in Vehicle-to-Grid Systems in Smart Cities

HICHAM KLAINA[1], (Student Member, IEEE), IMANOL PICALLO GUEMBE[2], PEIO LOPEZ-ITURRI[2,3], JOSÉ JAVIER ASTRAIN[3,4], LEYRE AZPILICUETA[5], (Senior Member, IEEE), OTMAN AGHZOUT[6], ANA VAZQUEZ ALEJOS[1], (Member, IEEE), AND FRANCISCO FALCONE[2,3], (Senior Member, IEEE)

[1]Department of Teoría de la Señal y comunicación, University of Vigo, 36310 Vigo, Spain
[2]Electric, Electronic and Communication Engineering Department, Public University of Navarre, 31006 Pamplona, Spain
[3]Institute of Smart Cities, Public University of Navarre, 31006 Pamplona, Spain
[4]Statistics, Computer Science and Mathematics Department, Public University of Navarra, 31006 Pamplona, Spain
[5]School of Engineering and Sciences, Tecnologico de Monterrey, Monterrey 64849, Mexico
[6]SIGL Laboratory, ENSA-Tetouan, Abdelmalek Essaadi University, Tetouan 93030, Morocco

Corresponding author: Hicham Klaina (hklaina@uvigo.es)

This work was supported in part by the 2017 Predoctoral Research Grant through the Xunta de Galicia and the Research Projects funded by the Ministerio de Ciencia, Innovación y Universidades, Gobierno de España through Ministerio de Ciencia, Innovación y Universidades (MCIU)/Agencia Estatal de Investigación (AEI)/Fondo Europeo de Desarrollo Regional (FEDER)/Union Europea (UE) under Grant TEC2017-85529-C03-3R and Grant RTI2018-095499-B-C31, and in part by the European Union's Horizon 2020 Research and Innovation Program (Stardust-Holistic and Integrated Urban Model for Smart Cities) under Grant N°774094.

ABSTRACT Recently, there has been growing attention to the power grid management due to the increasing concerns on global warming. With the advancement in electric vehicles (EV) industry and the evolution in batteries, EVs become an important contributor to the grid with capability of bidirectional power exchange with the grid. In this context, Vehicle-to-Grid (V2G) systems enable multiple functionalities between EVs and the corresponding aggregator. Thus, reliable, long-range communication capabilities between aggregator and EVs is compulsory. In this paper, wireless channel analysis for aggregator and electrical vehicle communication using Long-Range Wide Area Network (LoRaWAN) technology in V2G is presented, in order to test a low-cost solution with large coverage and reduced power consumption profile. Wireless channel and system-level measurements have been performed in a real urban scenario between EV's charging station in Pamplona (Spain) and a vehicle in motion using LoRaWAN 868 MHz devices. Wireless channel characterization is performed by implementing a full 3D urban scenario model, including elements such as buildings, vehicles, users and urban infrastructure such as lamp posts and benches. By means of in-house developed 3D Ray Launching algorithm with hybrid simulation capabilities, estimations of received power levels, signal to noise ratio and time domain parameters have been obtained, for the complete volume of the scenario under test in dense urban conditions. V2G end to end communication has been validated by implementing an intra-vehicle Controller Area Network-BUS (CAN BUS) data gathering system connected to the vehicle LoRaWAN transceiver and subsequently, to a cloud-based web service. The results show that the accurate deterministic based radio channel analysis enables to optimize the network design of LoRaWAN networks in a vehicular environment, considering inter-vehicular and infrastructure links, enabling scalable, low cost end to end data exchange for the deployment of ancillary V2G services.

INDEX TERMS Vehicle to grid (V2G), smart cities, LoRaWAN, 3D ray launching (3D-RL), radiofrequency characterization.

I. INTRODUCTION

The progressive adoption of Smart Cities and Smart Regions paradigms is promoting the implementation of Intelligent Transportation Systems (ITS). ITS have the capability of optimizing transportation services in terms of enhancing energy efficiency, reducing carbon footprint and improving quality of life of users and citizens in general. In this context, electrified transportation systems play a key role to reduce fossil fuel consumption and carbon emission. Electric vehi-

The associate editor coordinating the review of this manuscript and approving it for publication was Adnan M. Abu-Mahfouz.

cles (EV) can be classified as a function of their charging method (wired charging, static wireless charging, dynamic wireless charging), energy storage mechanisms (battery, supercapacitors, flywheel, hybrid energy storage) or their energy sources (hybrid electric vehicle, plug in hybrid electric vehicles) [1]. However, sustained growth of EV sales demands an increase in the amount of available electrical energy storage for use within future power systems [2]. Moreover, charging needs of EV are given partly by random variables, such as mobility and driver profiles. These variables affect EV charging demand allocation, biased by plug in period and by charging infrastructure availability [3]. In this sense, grid integration offers multiple opportunities towards more efficient operation, by taking advantage of the combination of embedded systems, electric grid and overall communication capabilities. This is enabled by the use of multiple communication links to support EV management and operation, such as Vehicle-to-Vehicle (V2V), Vehicle-to-Home (V2H) or Vehicle-to-Grid (V2G) [4]. In the case of medium electric voltage facilities, such as charging stations, V2G exhibit multiple features such as handling a large amount of EVs or enabling complex control mechanisms. This enables the development of multiple features, such as valley filling (EV charging at night when demand is low) and peak shaving (sending power back to the grid when demand is high), depending on the State of the Charge (SoC). These features provide power grid stability insurance. Demand based analysis solutions have also been implemented to optimize and balance power grid operation [5]–[12].

Within the context of EV communications, V2G is one of the main elements for energy handling and communication within the smart grid, exchanging information for two-way electric power transmission/consumption [13]. Moreover, it supports multiple ancillary services, such as user ID, payment or security [14]–[25]. An overview of V2G related applications is presented in Table 1.

In the context of V2G operation, the aggregator provides an interface between the grid control center (GCC) and the EVs. After receiving energy exchange information and related procedures from the GCC, the aggregator communicates with the EVs. Thus, with the aid of bi-directional chargers, charging or discharging operations can be performed, improving power grid operations in terms of power handling and reactive load compensation. Since the aggregator establishes direct communication links with the EVs, e.g. within a parking slot connected to the grid, a reliable long-range communication link between the aggregator and the EV should be guaranteed. There are several works related with V2G communication characteristics and quality of service considerations [26], [32].

In this sense, wireless link performance is limited by effects such as large-scale fading, small scale fading or Doppler shift, which directly affects system availability [33]–[35]. However, detailed wireless channel analysis for aggregator to EV communication and end to end validation in a Smart City environment hasn't been reported.

TABLE 1. V2G applications and services.

Ref	Description	Application/Service Provided [a]
[12]	Balancing Power Demand Through EV Mobility in V2G Mobile Energy Networks	The impact of mobility demand response management is analyzed, in order to optimize power demand balancing in relation with multiple EVs, considering bi-directional V2G communication links.
[14]	Battery Status Sensing Multicast for V2G Regulation in Smart Grid	Multiple sensor data extraction is exploited in order to analyze state of charge and battery status in order to optimize V2G regulation schemes.
[15]	Reliability-Oriented Reconfiguration of V2G Networks	Characterization of interference impact in plug in hybrid vehicle communication channel, considering different modulation/coding schemes.
[16]	Solving the Multivariant EV Routing Problem Incorporating V2G and G2V Options	A route optimization model is presented, based on the analysis and optimization of multiple variable, such as types of charging, time windows or load capacity among others, in order to present efficient routes.
[17]	Decentralized Cloud-SDN Architecture in Smart Grid: A Dynamic Pricing Model	Optimization of EV charging strategy is proposed, by obtaining vehicular data, based on a flexible SDN cloud system, supported by Network Function Virtualization. The proposed system enables gathering of real time user request and microgrid data transfer
[18]	Foud: Integrating Fog and Cloud for 5G-Enabled V2G Networks	A hybrid system based on a combination of permanent cloud and temporary fog is proposed for the provision of V2G services, supported on 5G network capabilities.
[19]	Online Scheduling for Hierarchical V2G System	A hierarchical tree like structure is proposed for the control of large sets of EV with multiple aggregators
[20]	Reactive Power Compensation Capabilities of V2G-Enabled Electric Vehicles	This study deals with reactive power compensation capabilities as an ancillary service in bidirectional battery chargers. Two different topologies are studied and validated at prototypes (direct battery and dc-dc buck type connection).
[21]	Wireless Authentication and TTCN-3basedTest Framework for ISO-15118 Wireless V2G Communication	A wireless authentication solution is proposed, in V2G communication context, based on WLAN links. ISO/IEC 15118 standard compliance of the proposed system is analyzed and validated.
[22]	Blockchain-Based Anonymous Rewarding Scheme for V2G Networks	A platform is proposed in order to provide to Battery Vehicles a framework in which security and privacy aspects are addressed by the use of multiple tools, including blockchain to implement rewarding based schemes.

This work presents wireless channel analysis in the context of V2G communications within a Smart City environment, focusing on the use of wireless sensor network transceivers, in order to explore the feasibility in the use of low cost,

TABLE 2. Wireless communication systems.

Wireless Communication System	LoRaWAN LoRa Alliance	SigFox ETSI	IEEE 802.15.4 ZigBee Alliance	4G LTE cat. 1 3GPP Rel. 8 (*)	4G LTE cat. M1 3GPP Rel. 13 (*)	4G LTE cat NB1 (NB-IoT) 3GPP Rel. 13 (*)
Frequency Band	433, 868 MHz (EU) 915 MHz (US)	868 MHz (EU) 902 MHz (US)	2.4 GHz (ISM) 868 MHz (EU) 915 MHz (US)	LTE bands	LTE bands	LTE bands
Data Rate	250 bps – 50 kbps (EU) 980 bps – 21.9 kbps (US)	100-600 bps (UL) 600 bps (DL)	20 kbps (EU) 40 kbps (US) 250 kbps (ISM)	5 Mbps (UL) 10 Mbps (DL)	1 Mbps (UL) 1 Mbps (DL)	1 Mbps (UL) 0.68 Mbps (DL)
Transmitted Power	14 dBm (EU) 27 dBm (US)	16 dBm (EU) 23 dBm (US)	8 dBm (max)	23 dBm	20-23 dBm	20-23 dBm
Power Consumption	Low	Low	Low	High	Medium	Low
Bandwidth	EU: 250/125 kHz UL/DL US: 500/500 kHz UL/DL	100 Hz (UL) 600 Hz (DL)	2 MHz	1.4-20 MHz	1.4 MHz	180-200 kHz
Sensitivity	-142 dBm	-126 dBm	-105 dBm	-	-117 dBm	-129 dBm
Cost (#Msgs/day)	Unlimited	140 Msgs/day	Unlimited	Unlimited	Unlimited	Unlimited
Range (km)	~ 3 km (urban) Star	3-10 km (urban) Star	300 m (LoS) 75-100 m (indoor) Mesh	5-20 km	2.5 km (urban)	1 km (urban)
References	https://loraalliance.orgabot-lorawan	https://build.sigfox.com/sigfox-device-radio-specifications	https://zigbeealliance.org/	(*) https://www.3gpp.org/		

widely deployable technology. Table 2 presents a comparison of wireless systems, which can be studied for V2G communications. Multiple wireless communication systems can be explored, from Public Land Mobile Networks (2G to 5G vehicle embedded transceivers), to auxiliary services within purpose specific V2X systems, such as Wireless Access for Vehicular Environments (WAVE) or Cooperative Intelligent Transportation Systems (C-ITS), to wireless sensor networks. Among the later, since communication takes place in complex urban scenarios with large density of obstacles and scatterers, Long-Range Wide Area Network (LoRaWAN) technology is a potential candidate for providing V2G connectivity, due to long range and low power consumption capabilities [36], [40]. In relation with potential limitations of LoRaWAN technology, it is worth noting that current network layouts employ a star topology, with direct connection to the gateway, not using meshing capabilities. The maximum achievable transmission rate is 50Kbps and in terms of delay and latency, values are moderate owing to constraints in radio duty cycle and the implementation of ALOHA MAC layer. Within wireless sensor network communication systems, other alternatives, such as ZigBee could be employed. However, usual receiver sensitivity levels are much higher (can be greater than 30 dB) as compared with LoRaWAN. Greater transmit power levels as well as mesh networking capabilities can aid in order to increase coverage levels, leading to higher node density as well as to overall higher energy consumption in the case of using ZigBee. This is given by the fact that meshing functionalities in general require more complex radio link handling functions, mainly within MAC layer and routing layer. In this way, devices operate as end-devices and also as routing elements, which in average increases energy consumption. This, however, provides higher levels of channel availability in the case of highly dynamic networks, owing to inherent reconfiguration capabilities. SigFox is another alternative for wireless connectivity, however, it has a limitation on the number of messages per day that can be sent, as a function of subscriber plans.

To this extent, in this work a LoRaWAN wireless communication system between the charging station and a vehicle is implemented. Wireless channel measurements have been performed between an existing public EV charging station and a moving vehicle in Pamplona (Spain) to analyze the coverage/capacity relations in the operational area of an aggregator. The LoRaWAN system setup has been implemented, connecting an intra-vehicle Controller Area Network-BUS (CAN BUS) data collector to 868 MHz LoRaWAN The Things Network (TTN) Uno and TTN gateway. End to end data collection and transfer has been analyzed, by considering transport of intra-vehicle data to an external data center. Intra-vehicle data is collected by means of an implemented prototype in which CAN BUS data is sent using a DFRobot/TTN

Uno platform connected to a TTN gateway for real data exchange within the scenario under analysis. Once the end to end data collection prototype has been implemented, V2G wireless propagation characteristics have been obtained. For this purpose, a deterministic 3D Ray Launching (3D-RL) algorithm, based on Geometrical Optics (GO) and Geometrical Theory of Diffraction (GTD) has been employed. The in-house implemented algorithm has been optimized in order to perform volumetric simulations in large scenarios. All the existing elements in the real scenario such as buildings, trees, streetlights and cars are taken into account (including frequency dispersive material properties such as conductivity and dielectric constant of all elements), in order to obtain accurate results. A detailed exploratory analysis that considers large-scale path loss, multipath metrics, comparison of measurements versus 3D-RL simulation and time domain characterization, is presented. The results provide coverage/capacity estimations for multiple types of wireless V2G communication links. A schematic description of the elements analyzed within the paper is depicted in Fig. 1.

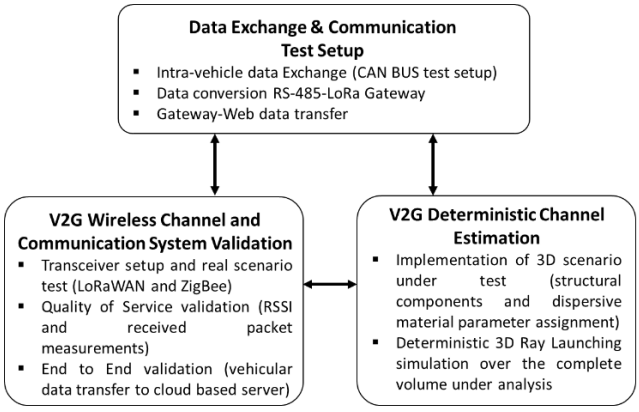

FIGURE 1. Schematic description of the V2G characterization performed: testbed implementation and validation, vehicular/infrastructure channel measurement and deterministic wireless channel validation.

The paper is organized as follows: Section II describes system level tests in relation with vehicle data exchange on the implemented LoRaWAN network, via CAN BUS data injection and extraction. Section III provides a description on V2G communication characterization, in terms of wireless system description and measurement results. In section IV, coverage/capacity analysis is presented with the aid of deterministic 3D-RL simulations of the city scenario under test. Finally, concluding remarks are presented in Section V.

II. VEHICLE INFORMATION DATA EXCHANGE

The integration of EV within the city infrastructure provides new opportunities in terms of energy handling, as well with other services within a Smart City framework. In this way, different ancillary services can be implemented, in which vehicular data can be combined with infrastructure driven information. In order to perform holistic system validation and the implementation of future services, a data exchange testbed is implemented. Intra-vehicle data is obtained, which in a further step can be exchanged in multiple communication links, as inter-vehicular links or towards local or cloud-based nodes. In this sense, intra-vehicle data collection and management is the initial element for validation. In this context, CAN (Controller Area Network) BUS is a widely used standard for intra-vehicular communication. CAN BUS is a serial bus standard allowing micro-controllers inside a vehicle to communicate without a host computer. Communication is performed by employing two CAN dedicated wires: CAN High (CAN H) and the CAN low (CAN L). Each module has a unique CAN ID that it uses when sending or receiving data. However, CAN bus protocol is still vulnerable and suffers from multiple security issues: i) confidentiality problems, as anyone can access to sensitive and private owner data and ii) integrity issues, as an attacker can inject data to the CAN bus without verification iii) availability issues, as a user can use the system without time limitation which gives lower priority nodes no chance for data transmission. To overcome these issues, some methods are adopted to secure the CAN bus. Network segmentation, encryption, authentication and intrusion detection. However, although that many actions have been undertaken to solve vulnerability issues, it's an open research topic [41]. Fig. 2 illustrates a simplified CAN BUS architecture and the implemented test setup for end to end validation. The on-board vehicle information provided by the CAN BUS, such as vehicle's speed and battery level, and the GPS location are then transmitted employing LoRaWAN communication system to the charging station. This real-time information is then transmitted to a cloud-based platform for storage and further processing. The charging station sends a downlink message, depending on the battery level of the EV and the availability of the parking lot.

To test end to end communication capabilities, a CAN BUS intra-vehicle data collection prototype has been implemented, using DFRobot CAN BUS shields v2.0, depicted in Fig. 2. These shields integrate an MCP2515 CAN BUS chip and have a CAN BUS transceiver function. An on-board DB9 interface is also integrated for an on-board diagnostic device or data logger through an OBD-II converter cable. Since Master/Slave operation in CAN isn't employed, the CAN shield connected to Arduino Uno will be sending data to the shield connected to the TTN Uno, and subsequently to the gateway. Moreover node 1 (the CAN shield connected to Arduino Uno) will be sending data to node 2 (the shield connected to the TTN Uno) through the CAN H and L in testbed. This provides a realistic approximation to real CAN bus functionality, with the data subsequently sent to the gateway via LoRaWAN for system validation.

Since TTN is based on Arduino Leonardo platform, a DFRobot CAN BUS Shield V2.0 was chosen, due to its compatibility with both Arduino Uno and Leonardo. Node 1 was programmed using Arduino IDE to exchange the CAN BUS data through CAN H and CAN L. The TTN is also programmed with Arduino IDE in order to forward the data received through LoRaWAN to the TTN gateway. In the TTN

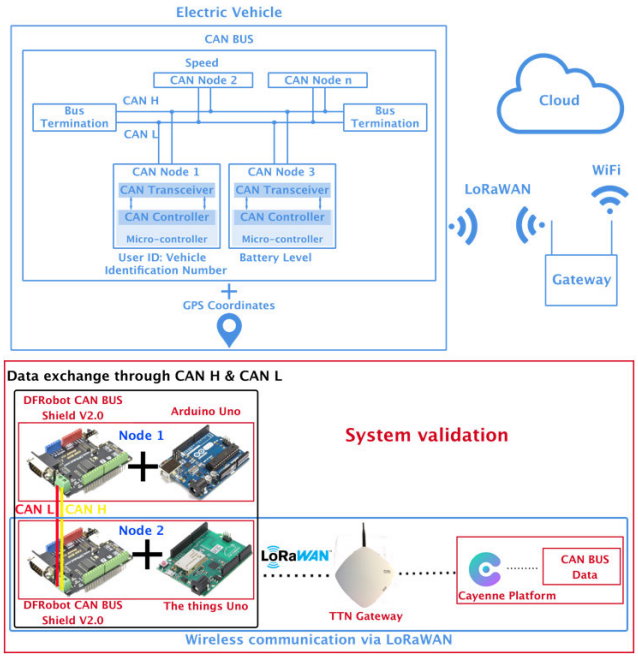

FIGURE 2. CAN BUS architecture schematic and external data transfer via wireless communication systems and the implemented testbed.

console, the payload is encoded with the Cayenne Low Power Payload (Cayenne LPP) in order to visualize real-time data. Moreover data is also stored enabling further analysis. The aim is to test end to end communication capabilities, employing LoRaWAN based wireless communication between the CAN BUS and the TTN gateway through the TTN Uno. Fig. 3 shows the implemented web-based dashboard, to analyze the received data by the TTN gateway from the CAN BUS. This model can be used for sending data such as battery level, electric power transmission/consumption, user ID (Vehicle Identification Number), payment information and other ancillary services, from an EV to the aggregator.

III. V2G WIRELESS COMMUNICATION CHANNEL MEASUREMENT CHARACTERIZATION

In order to evaluate quality of service metrics of wireless communication channels between a charging station and an EV, radio propagation characterization must be performed. For this purpose, measurements have been performed in the urban scenario under test, for LoRaWAN operating at 868 MHz in order to provide functionalities based on long range star topologies.

The CAN BUS shield connected to LoRaWAN TTN Uno 868 MHz is mounted in a moving vehicle, while the TTN gateway is attached to a public EV charging station at a height of 1.5 m. The location and trajectory of the scenario under test is within the urban area of the city of Pamplona, and the detail of the charging station is given in Fig. 4. The vehicle followed a trajectory within the vicinity of the charging station. This scenario exhibits a Non-Line of Sight (NLoS) maximum distance of 350 m between the charging station and the vehicle.

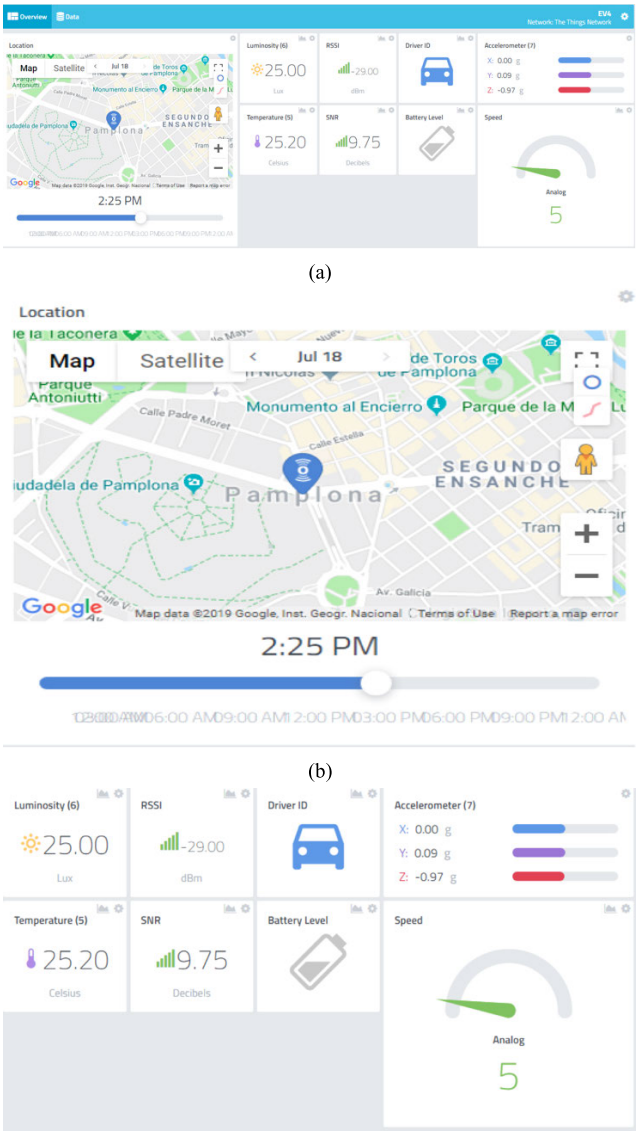

FIGURE 3. (a) End to End data communication setup, based on the TTN gateway and Cayenne dashboard; (b) Zoomed localization part; (c) Zoomed received data part.

The transmitted power is set to 14 dBm, whereas the receiver sensitivity is −148 dBm for the LoRaWAN transceivers. Received power levels have been measured with the aid of an Agilent N9912 Field Fox portable spectrum analyzer.

Once the scenario has been defined and system implementation has been performed, wireless system experimental validation is carried out. In the LoRaWAN experimental setup results were obtained for received packets, Received Signal Strength Indicator (RSSI) and Signal to Noise Ratio (SNR). Values were measured every 30 seconds from the starting point of the predefined path to the final destination. Fig. 5 shows experimental results for LoRaWAN wireless connectivity in terms of RSSI (Fig. 5a) and SNR (Fig. 5b). The measurements were taken along the path defined by a

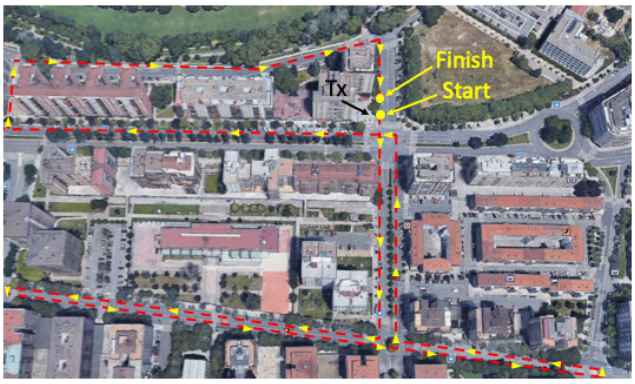

(a)

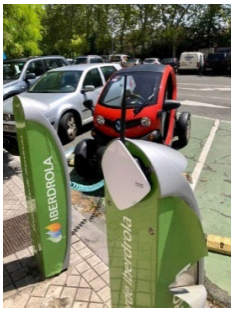

(b)

FIGURE 4. (a) Vehicle trajectory for both LoRaWAN measurements; (b) Detail of the LoRaWAN TTN gateway attached to the public charging station.

dashed red line (from point 'Start' to point 'Finish'). The results are depicted on the upper view of the scenario (with dimensions of 510 m in length and 285 m in width), following the color scale. Note that only the streets corresponding to the followed path are colored. From Fig. 5(a), it can be observed that the LoRaWAN node establishes a viable communication link (i.e., received power levels above receiver sensitivity threshold of −148 dBm) with the gateway throughout all the measured points.

The vehicle, by means of an automated script, sends packets to the gateway every 30s from the starting point in Fig. 5(a) at 9:50, until the finishing point at 10:37, while driving in low speed conditions (below 50 km/h, in accordance to applicable traffic regulation) to send packets from the maximum number of locations possible along the test path. In the field trials, 94 packets were received at the gateway, which corresponds a rate 100% of transmitted packets received.

The measurements points taken along the path can be divided into four different sections (numbered from 1 to 4 in Fig. 5a):

1) The first section is characterized by the absence of buildings, minimizing obstruction between transmitter-receiver links, resulting in higher RSSI values: between −12 dBm in the vicinity charging station and −63 dBm for at a distance of 250m in the road.
2) For the second section, in addition to trees, cars and streetlights, buildings obstruct direct line of sight after 70m, leading to lower RSSI values after that distance. The RSSI values vary between −44 dBm and −115 dBm for a 317 m road length.
3) In path section number 3, buildings are obstructing communication links along the 317 m road length. Thus, lower RSSI values, between −69 dBm and −116 dBm are observed
4) Finally, for section number 4, the presence of buildings and the distance between transmitter and receiver cause lower RSSI value (except for crossroads, due to the absence of buildings), resulting in a maximum RSSI value of −59 dBm and a minimum of −121 dBm for a road length of 465 m.

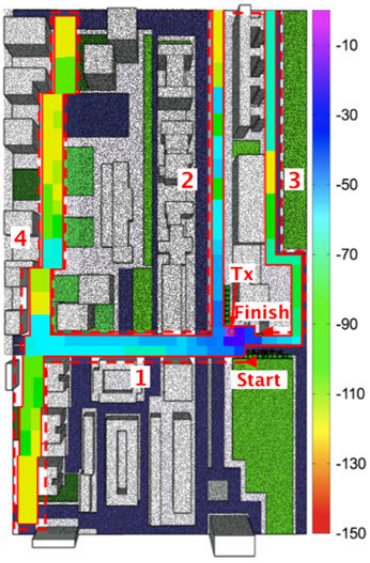

(a)

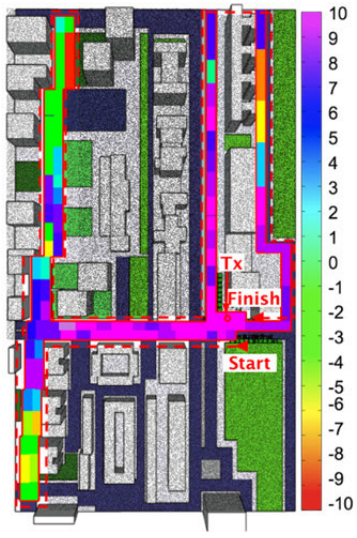

(b)

FIGURE 5. Experimental results for the wireless connectivity trials: (a) LoRaWAN RSSI results (in dBm); (b) LoRaWAN SNR results (in dB).

The ratio between the received power signal and the noise floor power level at the same measurements points are

presented in Fig. 5(b). The SNR varies between 10 dB and 6.5 dB in path section 1, 10 dB and 0.75 dB in section 2, 9.75 dB and −6.75 dB in path section 3 and between 8.75 and −9 dB in section 4.

IV. RADIOPLANNING DETERMINISTIC SIMULATION ANALYSIS OF V2G WIRELESS CONNECTIVITY

A. OVERVIEW OF WIRELESS CHANNEL ESTIMATION AND 3D-RL DESCRIPTION

In order to enable energy management as well as related ancillary applications, multiple functions and communications channels are defined, such as V2V, V2H or V2G [22]. Moreover, context aware environments such as Smart Cities or Smart Regions rely on heterogeneous network communication capabilities, which in the case of vehicular communications are generally described by vehicle to everything (V2X) links. Performance of vehicular related services depend on the underlying radio channel characteristics, mainly given by signal loss and interference conditions. Wireless channel characterization in vehicular environments poses different challenges, owing to inherent channel dynamics, the presence of vehicles, variable antenna heights and the influence of infrastructures and users within dense urban scenarios. Multiple approaches have been described in the literature in order to provide wireless channel characterization, based on geometry based stochastic models (generation of scatterer distribution following stochastic distributions), non-geometric based stochastic models (no specific geometric distribution is considered) and deterministic models (i.e., site specific characterization employing ray launching, ray tracing, or full wave electromagnetic simulation). In the case of geometric and non-geometric stochastic models, tapped delay line approaches have been experimented in order to obtain wideband channel characterization. Comprehensive surveys on wireless channel and physical layer characteristics and challenges within vehicular environments can be found in [42], [43]. A description of the employed models (described in references [44]–[50]) is outlined in Table 3.

In this work, an in-house implemented 3D Ray Launching (3D-RL) code is employed in order to perform wireless channel characterization of the V2G operation scenario. The 3D-RL code is based on geometric optics (GO) and uniform theory of diffraction (UTD) approach, in which predefined sources launch rays with a given angular resolution, for both horizontal and vertical planes with a given solid angle. The simulation scenario is implemented considering the volumetric description and frequency dispersive material properties of the elements within it, such as buildings, vehicles, trees, urban furnishings and simplified human body models. The effect of multipath propagation in complex environments such as the V2G operation scenario can result in a complex interference pattern. Multipath propagation components depend on the frequency band, the medium of transmission and the considered scenario. In this sense, multipath components have been considered in the 3D-RL algorithm by means of all reflected, refracted and diffracted rays. The resulting complex impulse response contains complete channel information. The principle of operation of the 3D-RL code is presented in Fig. 6.

TABLE 3. Wireless channel characterization in vehicular environments.

Ref	Description	Model Characteristics [a]
[44]	Time and Frequency Selective Channel models for Wireless LANs	Several road to vehicle and vehicle to vehicle models for application in 802.11p physical channel, based on tapped delay line model. The models (3 for road to vehicle and 3 for vehicle to vehicle) consider different operation scenarios (expressway, urban canyon, suburban street)
[46]	ETSI Technical Report TR 103 257-1 v1.1.1	Overview of different channel models with application in the 5.9GHz frequency band, with focus on V2X communication. Path loss models, tapped delay line models and geometry based stochastic models are presented, as well link level simulation models.
[47]	Improving the accuracy of environment-specific vehicular channel modeling	Localized environmental information is included in order to increase the accuracy. The characterization framework makes use of a tapped delay line model and the consideration of land covers within a geometry-based model.
[48-49]	Geometry-based vehicle-to-vehicle channel modeling for large-scale simulation	The authors describe the implementation of the Geometry-based Efficient propagation Model for V2V communication (GEMV^2) simulation tool. The tool considers LOS and different NLOS links, as a function of the scenario outline.
[50]	A Geometry-based Stochastic MIMO Model for Vehicle-to-Vehicle Communications	A channel characterization model is presented, based on an extensive measurement campaign in the 5.2 GHz frequency band. The proposed model can distinguish scatterer distributions, providing adequate characterization for SISO as well as MIMO channels.

The electric field E_i created by a transmitter antenna is calculated by [51]:

$$E_i^{\perp} = \sqrt{\frac{P_{\text{rad}} D_{\text{t}}(\theta_{\text{t}}, \emptyset_{\text{t}})\eta_0}{2\Pi}} \frac{e^{-\text{j}\beta_0 r}}{\text{r}} \text{X}^{\perp} L^{\perp} \quad (1)$$

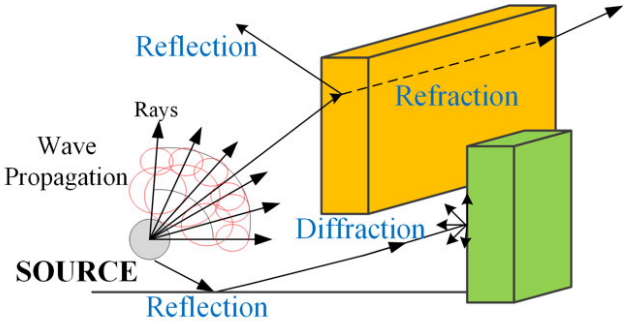

FIGURE 6. Principle of operation of the in-house developed 3D ray launching code.

$$E_i^{\parallel} = \sqrt{\frac{P_{\text{rad}} D_{\text{t}}(\theta_{\text{t}}, \emptyset_{\text{t}})\eta_0}{2\Pi}} \frac{e^{-\text{j}\beta_0 r}}{\text{r}} \text{X}^{\parallel} L^{\parallel} \quad (2)$$

where $\beta_0 = 2\pi f_{\text{c}}\sqrt{\varepsilon_0\mu_0}$, $\varepsilon_0 = 8.854 \cdot 10^{-12}$ F/m, $\mu_0 = 4\pi \cdot 10^{-7}$H/m and $\eta_0 = 120\pi$ ohms. P_{rad} is the radiated power of the transmitter antenna, $D_{\text{t}}(\theta_{\text{t}}, \emptyset_{\text{t}})$ is the directivity where rays are launched as defined in the spherical coordinate system at an elevation angle θ_{t} and an azimuth angle ϕ_{t}. $X^{\perp\parallel}$ and $L^{\perp\parallel}$are the polarization ratio and path loss coefficients for each polarization, r the distance in the free space and f_{c} the transmission frequency. Some shadowing areas can be caused by the GO approach in edges or discontinuities zones, which are analyzed with the diffraction coefficients on the obstacle's edges based on UTD. Thus, the diffracted field is calculated by [52]

$$E_{\text{UTD}}^{\perp} = e_0 \frac{e^{-\text{j}ks_1}}{s_1} D^{\perp} \sqrt{\frac{s_1}{s_2(s_1+s_2)}} e^{-\text{j}ks_2} \quad (3)$$

$$E_{\text{UTD}}^{\parallel} = e_0 \frac{e^{-\text{j}ks_1}}{s_1} D^{\parallel} \sqrt{\frac{s_1}{s_2(s_1+s_2)}} e^{-\text{j}ks_2} \quad (4)$$

where $D^{\perp\parallel}$are the diffraction coefficients for each polarization and s_1, s_2 are the distances from the source to the edge and from the edge to the receiver spatial point.

In order to reduce computational complexity, the simulation code has been optimized in order to include hybrid simulation options, such as neural network-based interpolators, diffraction estimation based on electromagnetic diffusion equation or collaborative filtering data base extraction. A full description of the code is available at [53]–[57], which has been tested and validated in different use cases and applications, including vehicular communications LoRaWAN technology and 5G [58]–[60].

B. V2G SCENARIO SIMULATION SETUP

The scenario under test has been recreated in the 3D-RL simulation environment implemented in Matlab. The elements of the scenario have been created individually in matrix form, defining the 3 dimensions element center coordinates, size and the material properties. For visualization purposes, the matrix elements are converted using Blender software to 3D models. For the transmitter, a specific matrix has been used to define the 3D coordinates of the antenna, the frequency range and the radiation patterns. Fig. 7(a) illustrates the aerial view of the scenario, while Fig. 7(b) shows the 3D model of the implemented scenario and Fig. 7(c) shows the side view of the location of the charging station.

The simulation scenario is 510 m long, 285 m wide and has a height of 50 m, with an overall volume of 7,267,500 m^3. All existing elements such as buildings, vehicles, streetlights, traffic lights, garbage containers, grass or benches have been considered. Table 4 presents material properties (relative permittivity and conductivity) of all the elements within the scenario. The dielectric constant and conductivity of the foliage of the trees is variable with humidity, as shown in equations (5) and (6) with the parameter h, where a humidity level

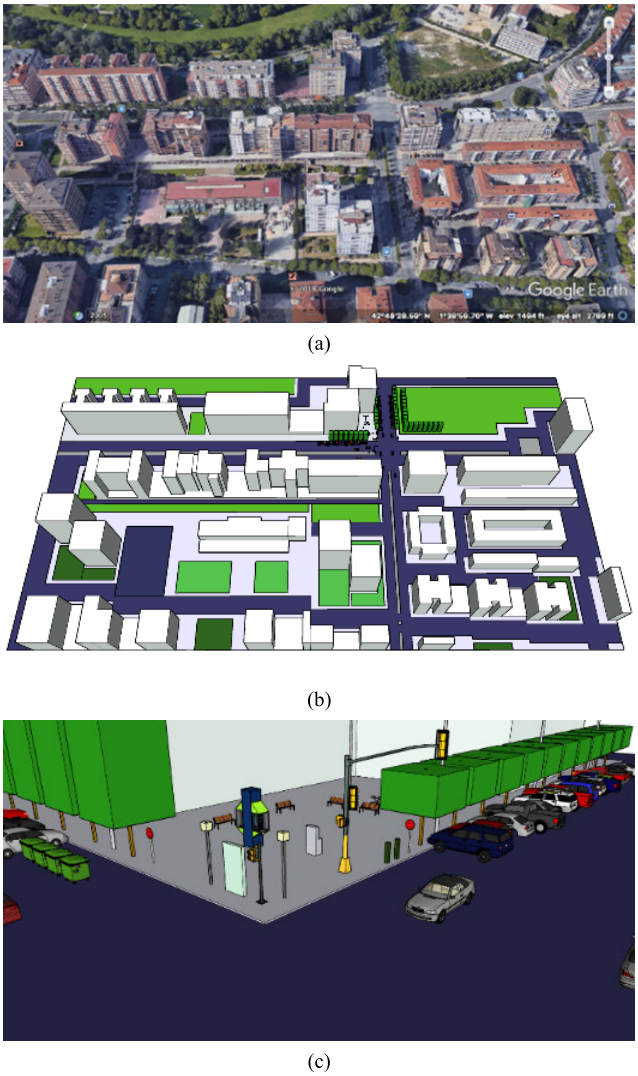

(a)

(b)

(c)

FIGURE 7. V2G urban scenario: (a) Google earth view; (b) 3D model view; (c) Side view from the 3D model.

of 20% has been considered [61]:

$$\varepsilon_{rfoliage} = 137h^3 - 69.688h^2 + 23.385h + 1.4984 \quad (5)$$

$$\sigma_{foliage} = 1.1541h^3 - 0.5489h^2 + 0.1669h - 0.0004 \quad (6)$$

TABLE 4. Material properties for the 3D ray launching algorithm.

Parameter	Relative Permittivity (ε_r)	Conductivity (σ) [S/m]
Metal	4.5	37.8*10^6
Plastic	8.5	0.02
PVC	4	0.12
Asphalt	5	0.7
Glass	6.06	0.11
Trunk tree	1.4	0.021
Tree foliage	Eq. (5)	Eq. (6)
Air	1	0
Brick wall	4.44	0.11
Grass	30	0.01

Simulation parameters have been selected as a function of convergence analysis criteria, given by the scenario volume [57]. In this way cuboids with a resolution of (6m, 6m, 2m) have been employed. Both vertical and horizontal ray launching angle resolution parameters are set to $\Delta\theta = \Delta\varphi = 1°$. Diffractions have been considered in this scenario and the number of reflections until extinction is 6. The transmitter has been placed at the point (X = 316.5m, Y = 215.5m, Z = 1.5m) corresponding to location of the gateway, with a transmit power of 14 dBm at 868 MHz. Fig. 8 presents bi-dimensional distribution of the estimated RF power levels, for a cut-plane at height of 1m (bottom of Fig. 8), as well as measurement results for RSSI values of LoRaWAN devices measured at 868 MHz (top of Fig. 8). Note that the measurement results are the same presented in Fig. 5a, but they are shown here for a better comparison with simulation results. The simulation results show good agreement with measurements, taking into account that the granularity of the simulation results is higher than those provided by the measurement points (i.e. the number of simulation points is higher than the measurement points).

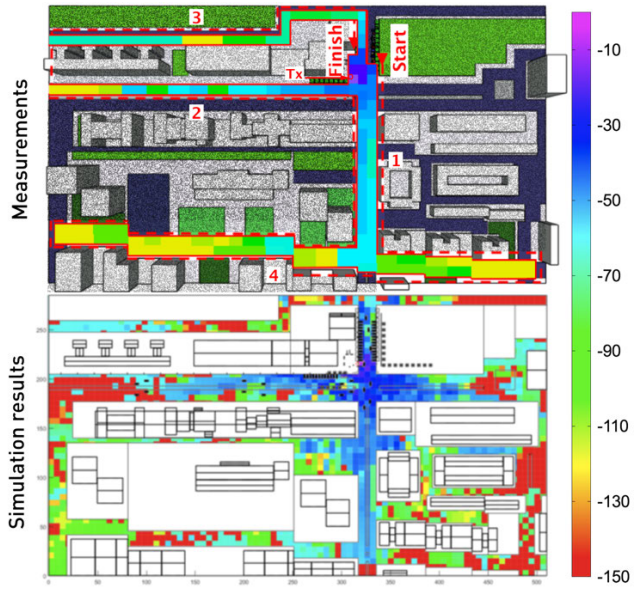

FIGURE 8. Comparison between measurement and simulation results, for the urban scenario under analysis and an operating frequency of 868 MHz (in dBm).

C. ANALYSIS OF WIRELESS CHANNEL SIMULATION

It is worth noting that simulation results have been obtained for the complete scenario volume, enabling the analysis for any location at any given height if required. From the results it can be seen that in general receiver sensitivity thresholds conditions are met, considering LoS as well as NLoS links. The bi dimensional coverage map exhibits certain differences, mainly given by difference in pixel size employed in the representation of the results. In order to provide a more accurate comparison of these results, Fig. 9(b) and (c) shows

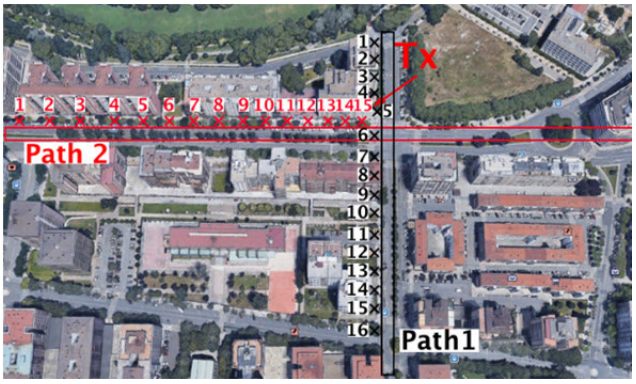

(a)

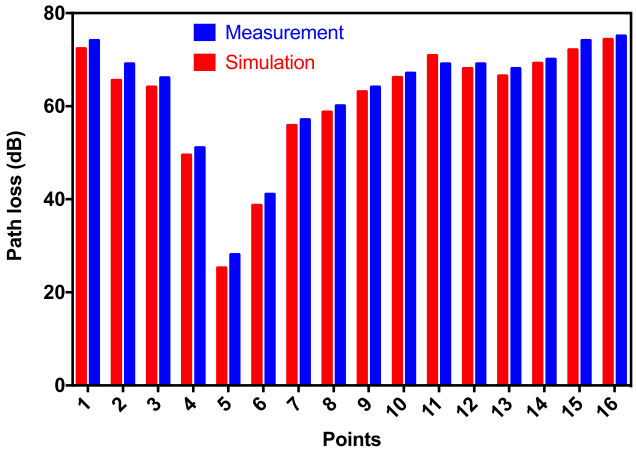

(b)

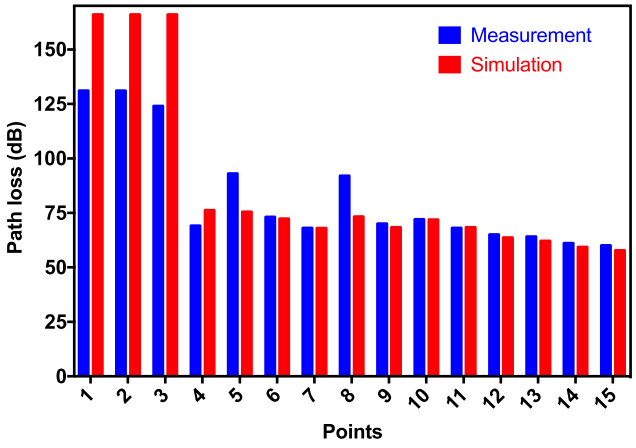

(c)

FIGURE 9. (a) Path 1 and 2 measurement points to be compared to the simulation results respectively in (b) and (c) in terms of path loss.

the difference between the estimated and the measured path loss in paths 1 and 2 considering the same antenna height.

A mean error $x = 2.24$ dB and a standard deviation $\sigma = 4.74$ dB is observed for the complete data set, except for the case of points 1, 2 and 3 of path 1, in which errors span from 35 dB to 43 dB. This is given by divergence effects,

for these points, which have an excess distance of 300m of the transmitting source and fall under NLoS conditions. In general, the results indicate that path losses comply with the receiver sensitivity levels, with a power margin in average above 30 dB for the scenario under test, assuring communication capabilities in the case of excess losses, given by conditions such as excess vehicle density or increased interference levels. Moreover, the simulation approach provides accurate received power level estimations, which benefits device/network design and planning processes.

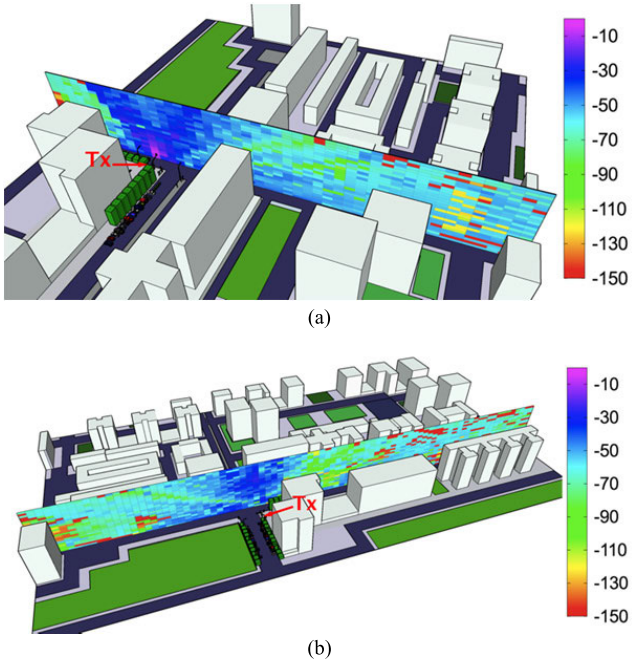

FIGURE 10. Estimated received power (in dBm) in vertical planes corresponding to paths (1) and (2) respectively.

As previously stated, results have been obtained for the complete scenario, providing also information relative to vertical planes. Fig. 10 shows the estimated received power in vertical planes in paths 1 and 2 respectively. This provides additional insight in relation with vehicular connectivity, in comparison with other approaches previously described in the literature, enabling transceiver locations for any given height conditions. In this way, it is feasible to analyze V2G connectivity with any other auxiliary infrastructure (e.g., locating communication equipment in lamp posts or other urban infrastructure), as well as with vehicles with different heights (such as buses or trucks) or with surrounding buildings. In order to provide further insight, Fig. 11 shows received power levels at $\boldsymbol{h_1 = 2m}$, $\boldsymbol{h_2 = 6m}$ and $\boldsymbol{h_3 = 10m}$ for paths 1 and 4. The maximum received power levels are depicted within the vicinity of the charging station for all heights, compared against minimum and maximum sensitivity thresholds for LoRaWAN transceivers. In general, except for specific locations at higher elevations (exceeding 10 m heights, given by the use of co-linear omni-directional antennas), coverage/capacity thresholds are met, enabling the location of transceivers at different heights. As a function of specific transceiver location requirements, alternative radiating antenna patterns could be considered (i.e, bi-lobular antennas, flat panel sector antennas), which could provide focused coverage patterns from taller locations towards vehicles, such as lamp posts or building facades.

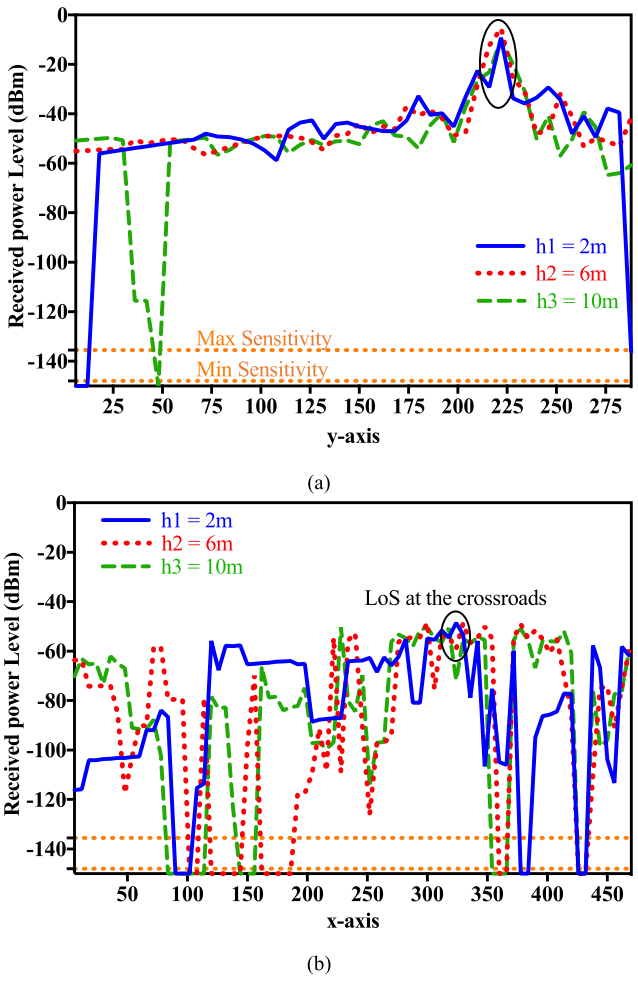

FIGURE 11. Received power level at different heights for: (a) Path 1; (b) Path 4.

The use of 3D-RL enables to obtain time domain channel characteristics for the scenario under analysis, such as power delay profiles (PDP), delay spread and time of flight estimations. Fig. 12(a) presents the estimated PDPs at 3 different locations identified as 1, 2 and 3 in the depicted scenario. Moreover, due to the relevance of multi height analysis as mentioned previously, PDPs at different heights are provided for the location 1: $\boldsymbol{h_1 = 2m}$, $\boldsymbol{h_2 = 6m}$ and $\boldsymbol{h_3 = 10m}$. Note that in order to show only physically measurable signals, the estimated multipath components corresponding to received power levels lower than LoRaWAN receiver sensitivity thresholds have been discarded (i.e. components under -148 dBm).

At location 1, corresponding to the crossroads close to the charging station, the first signal arrives at 62.6 ns for $\boldsymbol{h_1}$,

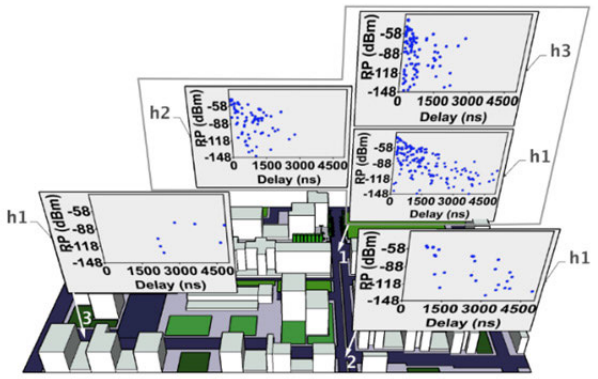

(a)

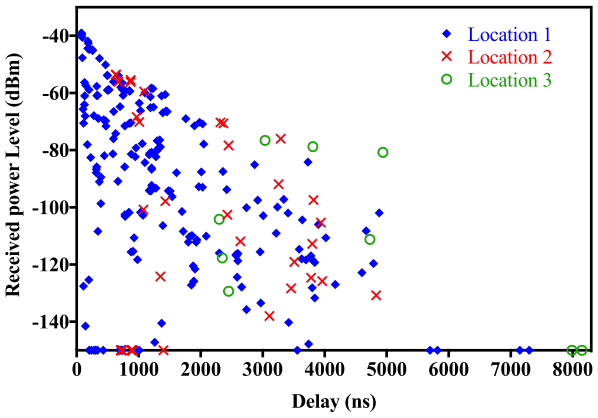

(b)

FIGURE 12. (a) Estimated power delay profile for locations 1, 2 and 3 and at different heights; (b) Comparison between the results at h_1 for the three locations.

64 ns for $\boldsymbol{h_2}$ and 85.3 ns for $\boldsymbol{h_3}$. The difference in time of flight between the first and the last multipath components is 7237.4 ns for $\boldsymbol{h_1}$, 2716 ns for $\boldsymbol{h_2}$ and 2424.7 ns for $\boldsymbol{h_3}$. The large number of multipath components and the large delay at $\boldsymbol{h_1}$ is caused by the presence of several metallic scatterers of less than 2m in the vicinity location 1. At location 2, the first multipath component arrives at 634 ns and the time delay is 4196 ns. Finally, at location 3, the first component arrives at 2300 ns, due to the NLoS propagation between the transmitter and the receiver. The delay between the first and the last multipath arrivals is 5850 ns. Furthermore, Fig. 12(b) presents a direct comparison between the estimated PDP at the 3 different locations at $\boldsymbol{h_1}$, showing the differences regarding the arrival time of the first component and the RF power level of the received components. All these results show how different the performance could be depending on the localization/deployment of the wireless devices and the importance of the radio planning tasks in such a complex environments.

Delay spread and Doppler spread can be calculated from PDP, for any given point in the scenario under analysis. PDP values are useful to determine the possibility of inter-symbol-interference (ISI) by a comparison to the symbol duration T_s that is calculated based on the devices setup parameters as indicated in (7) [62], [63]:

$$T_s = \frac{2^{SF}}{BW} \tag{7}$$

with SF the spreading factor of the chirp signal, and BW the channel bandwidth. For the present measurements it was considered $SF = 7$ and $BW = 125KHz$, resulting in $T_s = 102.4\mu s$. That is larger than the achieved PDP values ranging in the interval [2.7 μs, 7.2 μs]. This indicates that the radio channel can be considered as time-invariant, and it explains the low packet loss rate. Even for the largest BW value available in LoRA, 500 KHz, $T_s = 25.6\mu s$ would be enough to avoid ISI, allowing large coverage links.

V. CONCLUSION

In this work, V2G communication capabilities, considering intra-vehicle data gathering and exchange, towards aggregators as well as to other potential ancillary services has been presented. Intra-vehicle data has been collected via a CAN BUS prototype, connected with LoRaWAN transceivers and gateway, providing end to end communication to web services in a cloud-deployed architecture. Wireless communication has been tested for LoRaWAN at 868MHz. Detailed wireless channel characterization has been performed for the complete volume of the scenario under analysis with the aid of an in house 3D-RL code, optimized in order to obtain power distribution, interference characterization and time domain parameters in such large and complex environment. Simulation and measurement results show good agreement, characterizing all the potential measurement points in a volumetric fashion. In this way, it is possible to consider multiple type of communication links and location of communication equipment within the infrastructure, such as in lampposts at different heights, bus stops or buildings, among others. The significant improvement of using the in-house 3D-RL algorithm for V2G wireless communication links versus other approaches is the provided additional insight in relation with vehicular connectivity, enabling transceiver locations for any given height conditions. End to end communication has been tested with moving vehicles communicating to a public EV charging stations, with packet success rate of 100% in the case of using LoRaWAN transceivers. The proposed methodology enables the design of multi-service communication systems, applicable in V2G as well as in other vehicular related applications in complex urban environments. The main advantage of considering LoRaWAN is receiver sensitivity, of -148 dBm, much higher than nominal sensitivity of ZigBee and Bluetooth receivers in the range of -125 dBm to -90 dBm, respectively [64]. Even for scenarios under harsher multipath conditions LoRaWAN would enable to adjust parameters such as SF, BW, and coding efficiency R to counteract quality loss [62], [63].

REFERENCES

[1] C. T. Rim and C. Mi, *Wireless Power Transfer for Electric Vehicles and Mobile Devices*. Hoboken, NJ, USA: Wiley, 2017.

[2] A. S. Hassan, N. Jenkins, L. M. Cipcigan, E. S. Xydas, and C. E. Marmaras, "Integration of wind power using V2G as a flexible storage," in *Proc. IET Conf. Power Unity, Whole Syst. Approach*, London, U.K., 2013, pp. 1–5.

[3] R. Garcia-Valle and J. A. Pecas Lopes, *Electric Vehicle Integration into Modern Power Networks*. New York, NY, USA: Springer, 2013.

[4] C. Liu, K. T. Chau, D. Wu, and S. Gao, "Opportunities and challenges of vehicle-to-home, vehicle-to-vehicle, and vehicle-to-grid technologies," *Proc. IEEE*, vol. 101, no. 11, pp. 2409–2427, Nov. 2013.

[5] H. Ramadan, A. Ali, M. Nour, and C. Farkas, "Smart charging and discharging of plug-in electric vehicles for peak shaving and valley filling of the grid power," in *Proc. 20th Int. Middle East Power Syst. Conf. (MEPCON)*, Cairo, Egypt, Dec. 2018, pp. 735–739.

[6] D. Steward, "Critical elements of vehicle-to-grid (V2G) economics," Nat. Renew. Energy Lab., U.S. Dept. Energy, Washington, DC, USA, Tech. Rep. NREL/TP-5400-69017, 2017. [Online]. Available: https://www.nrel.gov/docs/fy17osti/69017.pdf

[7] T. U. Daim, X. Wang, K. Cowan, and T. Shott, "Technology roadmap for smart electric vehicle-to-grid (V2G) of residential chargers," *J. Innov. Entrepreneurship*, vol. 5, no. 1, p. 15, Dec. 2016, doi: 10.1186/s13731-016-0043-y.

[8] M. Liu, Y. Shi, and H. Gao, "Aggregation and charging control of PHEVs in smart grid: A cyber–physical perspective," *Proc. IEEE*, vol. 104, no. 5, pp. 1071–1085, May 2016.

[9] J. J. Escudero-Garzás, A. García-Armada, and G. Seco-Granados, "Fair design of plug-in electric vehicles aggregator for V2G regulation," *IEEE Trans. Veh. Technol.*, vol. 61, no. 8, pp. 3406–3419, Oct. 2012.

[10] E. L. Karfopoulos, K. A. Panourgias, and N. D. Hatziargyriou, "Distributed coordination of electric vehicles providing V2G regulation services," *IEEE Trans. Power Syst.*, vol. 31, no. 4, pp. 2834–2846, Jul. 2016.

[11] A. Y. S. Lam, K.-C. Leung, and V. O. K. Li, "Capacity estimation for vehicle-to-grid frequency regulation services with smart charging mechanism," *IEEE Trans. Smart Grid*, vol. 7, no. 1, pp. 156–166, Jan. 2016.

[12] R. Yu, W. Zhong, S. Xie, C. Yuen, S. Gjessing, and Y. Zhang, "Balancing power demand through EV mobility in vehicle-to-grid mobile energy networks," *IEEE Trans. Ind. Informat.*, vol. 12, no. 1, pp. 79–90, Feb. 2016.

[13] S. Vadi, R. Bayindir, A. M. Colak, and E. Hossain, "A review on communication standards and charging topologies of V2G and V2H operation strategies," *Energies*, vol. 12, no. 19, p. 3748, Sep. 2019.

[14] G. Li, J. Wu, J. Li, T. Ye, and R. Morello, "Battery status sensing software-defined multicast for V2G regulation in smart grid," *IEEE Sensors J.*, vol. 17, no. 23, pp. 7838–7848, Dec. 2017.

[15] A. Kavousi-Fard, M. A. Rostami, and T. Niknam, "Reliability-oriented reconfiguration of vehicle-to-grid networks," *IEEE Trans. Ind. Informat.*, vol. 11, no. 3, pp. 682–691, Jun. 2015.

[16] A. Abdulaal, M. H. Cintuglu, S. Asfour, and O. A. Mohammed, "Solving the multivariant EV routing problem incorporating V2G and G2V options," *IEEE Trans. Transport. Electrific.*, vol. 3, no. 1, pp. 238–248, Mar. 2017.

[17] D. A. Chekired, L. Khoukhi, and H. T. Mouftah, "Decentralized cloud-SDN architecture in smart grid: A dynamic pricing model," *IEEE Trans. Ind. Informat.*, vol. 14, no. 3, pp. 1220–1231, Mar. 2018.

[18] M. Tao, K. Ota, and M. Dong, "Foud: Integrating fog and cloud for 5G-enabled V2G networks," *IEEE Netw.*, vol. 31, no. 2, pp. 8–13, Mar./Apr. 2017.

[19] X. Chen, K.-C. Leung, A. Y. S. Lam, and D. J. Hill, "Online scheduling for hierarchical vehicle-to-grid system: Design, formulation, and algorithm," *IEEE Trans. Veh. Technol.*, vol. 68, no. 2, pp. 1302–1317, Feb. 2019.

[20] G. Buja, M. Bertoluzzo, and C. Fontana, "Reactive power compensation capabilities of V2G-enabled electric vehicles," *IEEE Trans. Power Electron.*, vol. 32, no. 12, pp. 9447–9459, Dec. 2017.

[21] Z. Jakó, Á. Knapp, and N. El Sayed, "Wireless authentication solution and TTCN-3 based test framework for ISO-15118 wireless V2G communication," *Infocommun. J.*, vol. 11, no. 2, pp. 39–47, Jun. 2019.

[22] H. Wang, Q. Wang, D. He, Q. Li, and Z. Liu, "BBARS: Blockchain-based anonymous rewarding scheme for V2G networks," *IEEE Internet Things J.*, vol. 6, no. 2, pp. 3676–3687, Apr. 2019.

[23] M. Wang, Y. Mu, Q. Shi, H. Jia, and F. Li, "Electric vehicle aggregator modeling and control for frequency regulation considering progressive state recovery," *IEEE Trans. Smart Grid*, early access, Mar. 19, 2020, doi: 10.1109/TSG.2020.2981843.

[24] C. D. Korkas, S. Baldi, S. Yuan, and E. B. Kosmatopoulos, "An adaptive learning-based approach for nearly optimal dynamic charging of electric vehicle fleets," *IEEE Trans. Intell. Transp. Syst.*, vol. 19, no. 7, pp. 2066–2075, Jul. 2018.

[25] N. I. Nimalsiri, C. P. Mediwaththe, E. L. Ratnam, M. Shaw, D. B. Smith, and S. K. Halgamuge, "A survey of algorithms for distributed charging control of electric vehicles in smart grid," *IEEE Trans. Intell. Transp. Syst.*, early access, Oct. 2, 2019, doi: 10.1109/TITS.2019.2943620.

[26] J. Park, H. Kim, and J.-Y. Choi, "Improving TCP performance in vehicle-to-grid (V2G) communication," *Electronics*, vol. 8, no. 11, p. 1206, 2019.

[27] J. Donoghue and A. J. Cruden, "Whole system modelling of V2G power network control, communications and management," in *Proc. World Electr. Vehicle Symp. Exhib. (EVS27)*, Barcelona, Spain, Nov. 2013, pp. 1–9.

[28] S. Kumar and R. Y. Udaykumar, "IEEE 802.16–2004(WiMAX) protocol for grid control center and aggregator communication in V2G for smart grid application," in *Proc. IEEE Int. Conf. Comput. Intell. Comput. Res.*, Enathi, India, Dec. 2013, pp. 1–4.

[29] B. Kwon, C. Park, J. Lee, and S. Park, "Timeout notification method for efficient V2G communication," in *Proc. 20th Asia–Pacific Conf. Commun. (APCC)*, Pattaya, Thailand, Oct. 2014, pp. 376–381.

[30] A. Krivchenkov and R. Saltanovs, "Analysis of wireless communications for V2G applications using WPT technology in energy transfer to mobile objects," in *Proc. 56th Int. Sci. Conf. Power Electr. Eng. Riga Tech. Univ. (RTUCON)*, Riga, Latvia, Oct. 2015, pp. 1–4.

[31] Y. Li, G. Yu, J. Liu, and F. Deng, "Design of V2G auxiliary service system based on 5G technology," in *Proc. IEEE Conf. Energy Internet Energy Syst. Integr. (EI2)*, Beijing, China, Nov. 2017, pp. 1–6.

[32] J. Wang, P. Zeng, X. Jin, F. Kong, Z. Wang, D. Li, and M. Wan, "Software defined Wi-V2G: A V2G network architecture," *IEEE Intell. Transp. Syst. Mag.*, vol. 10, no. 2, pp. 167–179, Apr. 2018.

[33] J. D. Parsons, *The Mobile Radio Propagation Channel*. Hoboken, NJ, USA: Wiley, 2000.

[34] X. Yin and X. Cheng, *Propagation Channel Characterization, Parameter Estimation, and Modeling for Wireless Communications*. Singapore: Wiley, 2016.

[35] Z. Yun and M. F. Iskander, "Ray tracing for radio propagation modeling: Principles and applications," *IEEE Access*, vol. 3, pp. 1089–1100, 2015.

[36] P. Jörke, S. Böcker, F. Liedmann, and C. Wietfeld, "Urban channel models for smart city IoT-networks based on empirical measurements of LoRa-links at 433 and 868 MHz," in *Proc. IEEE 28th Annu. Int. Symp. Pers., Indoor, Mobile Radio Commun. (PIMRC)*, Montreal, QC, Canada, Oct. 2017, pp. 1–6.

[37] L. Oliveira, J. P. C. J. Rodrigues, A. S. Kozlov, A. L. R. Rabêlo, and V. Furtado, "Performance assessment of long-range and Sigfox protocols with mobility support," *Int. J. Commun. Syst.*, vol. 32, Aug. 2019, Art. no. e3956, doi: 10.1002/dac.3956.

[38] C. F. de Oliveira, J. P. C. J. Rodrigues, A. L. R. Rabêlo, and S. Mumtaz, "Performance delay comparison in random access procedure for NB-IoT, LoRa, and SigFox IoT protocols," in *Proc. 1st Sustain. Cities Latin Amer. (IOT-SCLA)*, Arequipa, Peru, Aug. 2019, pp. 1–6.

[39] W. R. Da Silva, L. Oliveira, N. Kumar, R. A. L. Rabêlo, C. N. M. Marins, and J. J. P. C. Rodrigues, "An Internet of Things tracking system approach based on LoRa protocol," in *Proc. IEEE Global Commun. Conf. (GLOBECOM)*, Abu Dhabi, UAE, Dec. 2018, pp. 1–7.

[40] A. Ouya, B. M. De Aragon, C. Bouette, G. Habault, N. Montavont, and G. Z. Papadopoulos, "An efficient electric vehicle charging architecture based on LoRa communication," in *Proc. IEEE Int. Conf. Smart Grid Commun. (SmartGridComm)*, Oct. 2017, pp. 381–386.

[41] M. Bozdal, M. Samie, S. Aslam, and I. Jennions, "Evaluation of CAN bus security challenges," *Sensors*, vol. 20, no. 8, p. 2364, Apr. 2020.

[42] C.-X. Wang, X. Cheng, and D. Laurenson, "Vehicle-to-vehicle channel modeling and measurements: Recent advances and future challenges," *IEEE Commun. Mag.*, vol. 47, no. 11, pp. 96–103, Nov. 2009.

[43] W. Viriyasitavat, M. Boban, H.-M. Tsai, and A. Vasilakos, "Vehicular communications: Survey and challenges of channel and propagation models," *IEEE Veh. Technol. Mag.*, vol. 10, no. 2, pp. 55–66, Jun. 2015.

[44] G. Acosta-Marum and D. Brunelli, "Six time-and frequency-selective empirical channel models for vehicular wireless LANs," *IEEE Vehic. Tech. Mag.*, vol. 2, no. 4, pp. 4–11, Dec. 2007.
[45] *Standard for Wireless Local Area Networks Providing Wireless Communications while in Vehicular Environment*, IEEE Standard IEEE P802.11p/D2.01, Mar. 2007.
[46] *Intelligent Transport Systems (ITS); Access Layer; Part 1: Channel Models for the 5,9 GHz Frequency Band*, document TR 103 257-1, v1.1.1, ETSI, May 2019.
[47] X. Wang, E. Anderson, P. Steenkiste, and F. Bai, "Improving the accuracy of environment-specific channel modeling," *IEEE Trans. Mobile Comput.*, vol. 15, no. 4, pp. 868–882, Apr. 2016.
[48] M. Boban, J. Barros, and O. K. Tonguz, "Geometry-based vehicle-to-vehicle channel modeling for large-scale simulation," *IEEE Trans. Veh. Technol.*, vol. 63, no. 9, pp. 4146–4164, Nov. 2014.
[49] *GEMV2 Channel Model*. Accessed: May 10, 2020. [Online]. Available: http://vehicle2x.net/
[50] J. F. K. Tufvesson, N. Czink, A. Paier, C. Dumard, T. Zemen, C. Mecklenbräuker, and A. Molisch, "A geometry-based stochastic MIMO model for vehicle-to-vehicle communications," *IEEE Trans. Wireless Commun.*, vol. 8, no. 7, pp. 3646–3657, Jul. 2009.
[51] A. C. Aznar, *Antenas*. Barcelona, Spain: Edicions UPC, 1993.
[52] S. Salous, *Radio Propagation Measurement and Channel Modelling*, 1st ed. London, U.K.: Wiley, 2013.
[53] L. Azpilicueta, M. Rawat, K. Rawat, F. M. Ghannouchi, and F. Falcone, "A ray launching-neural network approach for radio wave propagation analysis in complex indoor environments," *IEEE Trans. Antennas Propag.*, vol. 62, no. 5, pp. 2777–2786, May 2014.
[54] L. Azpilicueta, F. Falcone, and R. Janaswamy, "Hybrid computational techniques: Electromagnetic propagation analysis in complex indoor environments," *IEEE Antennas Propag. Mag.*, vol. 61, no. 6, pp. 20–30, Dec. 2019.
[55] F. Casino, L. Azpilicueta, P. López-Iturri, E. Aguirre, F. Falcone, and A. Solanas, "Optimized wireless channel characterization in large complex environments by hybrid ray launching-collaborative filtering approach," *IEEE Antennas Wireless Propag. Lett.*, vol. 16, pp. 780–783, 2017.
[56] L. Azpilicueta, M. Rawat, K. Rawat, F. Ghannouchi, and F. Falcone, "Convergence analysis in deterministic 3D ray launching radio channel estimation in complex environments," *Appl. Comput. Electromagn. Soc. J.*, vol. 29, no. 4, pp. 256–271, 2014.
[57] L. Azpilicueta, C. Vargas-Rosales, and F. Falcone, "Intelligent vehicle communication: Deterministic propagation prediction in transportation systems," *IEEE Veh. Technol. Mag.*, vol. 11, no. 3, pp. 29–37, Sep. 2016.
[58] P. Fraga-Lamas, M. Celaya-Echarri, P. Lopez-Iturri, L. Castedo, L. Azpilicueta, E. Aguirre, M. Suárez-Albela, F. Falcone, and T. M. Fernández-Caramés, "Design and experimental validation of a LoRaWAN fog computing based architecture for IoT enabled smart campus applications," *Sensors*, vol. 19, no. 15, p. 3287, Jul. 2019.
[59] F. A. Rodríguez-Corbo, L. Azpilicueta, M. Celaya-Echarri, P. López-Iturri, I. Picallo, F. Falcone, and A. V. Alejos, "Millimeter wave spatial channel characterization for vehicular communications," in *Proc. 6th Int. Electron. Conf. Sensors Appl.*, Nov. 2019, pp. 1–6.
[60] M. Celaya-Echarri, L. Azpilicueta, P. Lopez-Iturri, F. Falcone, M. G. Sanchez, and A. V. Alejos, "Validation of 3D simulation tool for radio channel modeling at 60 GHz: A meeting point for empirical and simulation-based models," *Measurement*, vol. 163, Oct. 2020, Art. no. 108038.
[61] V. V. Komarov. *Handbook of Dielectric and Thermal Properties of Materials at Microwave Frequencies*. Boston, MA, USA: Artech House, 2012.
[62] K. Staniec and M. Kowal, "LoRa performance under variable interference and heavy-multipath conditions," *Wireless Commun. Mobile Comput.*, vol. 2018, pp. 1–9, Apr. 2018.
[63] *Electromagnetic Compatibility and Radio Spectrum Matters (ERM); Frequency-Agile Generic Short Range Devices Using Listen-Before-Transmit (LBT)*, document TR 102 313, V1.1.1 (2004-07), ETSI, 2004.
[64] M. Centenaro, L. Vangelista, A. Zanella, and M. Zorzi, "Long-range communications in unlicensed bands: The rising stars in the IoT and smart city scenarios," *IEEE Wireless Commun.*, vol. 23, no. 5, pp. 60–67, Oct. 2016.

HICHAM KLAINA (Student Member, IEEE) received the master's degree in networks and telecommunications engineering from the National School of Applied Sciences of Tetouan (ENSATé), Morocco, in 2016. He is currently pursuing the Ph.D. degree in telecommunications engineering with the University of Vigo, Spain. He has over ten contributions in indexed international journals and conference contributions. His research interests include smart agriculture, near-ground radio propagation, wireless sensor networks, vehicular communication, channel modeling, the IoT networks and devices, RFID, and 5G communication systems. He received the Best Final Year Project Award from the National School of Applied Sciences of Tetouan, in 2016, the 2017 Predoctoral Research Grant supported by the Xunta de Galicia, and the ECSA-4 Best Paper Award, in 2017.

IMANOL PICALLO GUEMBE received the bachelor's degree in telecommunications engineering from the Public University of Navarre (UPNA), in 2016, the master's degree in telecommunication engineering from the Charles III University of Madrid (UC3M), in 2019, and the Ph.D. degree in communication engineering from UPNA. He worked with Zener Group Company, as a Developer. He is currently working on several public and privately funded research projects. He has over ten contributions in indexed international journals and conference contributions. His research interests include radio propagation in homogeneous environments, human body interference analysis, wireless sensor networks, the IoT networks, and 5G communications systems. He received the ISSI 2019 Best Paper Award.

PEIO LOPEZ-ITURRI received the degree in telecommunications engineering, the master's degree in communications, and the Ph.D. degree in communication engineering from the Public University of Navarre (UPNA), Pamplona, Navarre, in 2011, 2012, and 2017, respectively. In 2019, he was a Researcher with Tafco Metawireless. He is currently affiliated with the Institute for Smart Cities (ISC), UPNA. He has worked in ten different public and privately funded research projects. He has over 150 contributions in indexed international journals, book chapters, and conference contributions. His research interests include radio propagation, wireless sensor networks, electromagnetic dosimetry, modeling of radio interference sources, mobile radio systems, wireless power transfer, the IoT networks and devices, 5G communication systems, and EMI/EMC. He received the ECSA 2014 Best Paper Award, the IISA 2015 Best Paper Award, the 2018 Best Spanish Ph.D. thesis in Smart Cities, CAEPIA, in 2018 (Third Prize), sponsored by the Spanish Network on Research for Smart Cities CI-RTI and Sensors, and the ISSI 2019 Best Paper Award.

JOSÉ JAVIER ASTRAIN received the degree in telecommunications engineering and the Ph.D. degree in computer science from the Public University of Navarre (UPNA), Spain, in 1999 and 2004, respectively. He is currently a Lecturer with UPNA. He has worked in more than 60 different public and privately funded research projects. He is the coauthor of two Spanish patents. His current research interests include wireless sensor networks, distributed systems, and cloud computing. He is a member of the Institute of Smart Cities, UPNA. He received the Premio Talgo 2012 for Technological Innovation.

LEYRE AZPILICUETA (Senior Member, IEEE) received the degree in telecommunications engineering, the master's degree in communications, and the Ph.D. degree in telecommunication technologies from the Public University of Navarre (UPNa), Spain, in 2009, 2011, and 2015, respectively. In 2010, she was with the Research and Development Department, RFID Osés, as a Radio Engineer. She is currently an Associate Professor and a Researcher with the Tecnologico de Monterrey, Monterrey, Mexico. She has over 150 contributions in relevant journals and conference publications. Her research interests include radio propagation, mobile radio systems, ray tracing, and channel modeling. She was a recipient of the IEEE Antennas and Propagation Society Doctoral Research Award, in 2014, the Young Professors and Researchers Santander Universities 2014 Mobility Award, the ECSA 2014 Best Paper Award, the IISA 2015 Best Paper Award, the ISSI 2019 Best Paper Award, the Best Ph.D. from the Colegio Oficial de Ingenieros de Telecomunicación, in 2016, and the N2Women Rising Stars in Computer Networking and Communications 2018 Award.

OTMAN AGHZOUT was born in Tétouan, Morocco. He received the Ph.D. degree in telecommunications engineering from the High School of Telecommunications Engineering, University of Las Palmas de Gran Canaria, Spain, in January 2002. He was a Research Student with the Microwave Group, Department of Electronics and Electromagnetism, University of Seville, Spain, from 1996 to 1999. In January 2002, he joined the Medical Technology Center, University Hospital of GC, where he worked in medical engineering applications, for a period of two years, from 2002 to 2004. In 2009, he joined the National School of Applied Sciences, AbdelMalek Essaadi University, Tétouan, as an Associate Professor with the Department of Telecommunication Engineering. Since 2019, he has been with the Department of Computer Science Engineering. More than ten years, he has taught several courses on electromagnetism waves, waveguides, transmission lines, RF propagation, satellite telecommunication, antennas, microwave circuit theory, and related topics to graduate students. He has authored or coauthored over 70 technical papers published in international journals or presented at international conferences. His research interests include printed microwave passive and active circuits, filters, antenna designs, medical imaging systems, theory of characteristic modes analysis, the Internet of Things, and smart cities applications. He was a recipient of the Research Scholarship of UNELCO, in 2000.

ANA VAZQUEZ ALEJOS (Member, IEEE) received the M.S. and Ph.D. degrees from the University of Vigo, Spain, in 2000 and 2006, respectively. She completed the Ph.D. thesis on the radio channel characterization for the millimetre-wave frequencies. In 2009, she was granted with the Marie Curie International Outgoing Fellowship, carrying out the outgoing phase with the Klipsch School of ECE, New Mexico State University, Las Cruces, NM, USA, with a research focused on measurement and modeling of propagation through dispersive media and radar waveform generation. She is currently an Associate Professor with the Department of Signal Theory and Communications, University of Vigo. Her research interests include radio propagation, communication electronics, radio channel modeling, multimedia wireless systems, waveform and noise code design, and radar and antennas. Her master's thesis received the Ericcson Award from the Spanish Association of Electrical Engineers, as the Best Multimedia Wireless Project, in 2002. She served as an Associate Editor for Elsevier AEUE Journal. She is a Reviewer of several the IEEE and IET journals.

FRANCISCO FALCONE (Senior Member, IEEE) received the degree in telecommunication engineering and the Ph.D. degree in communication engineering from the Universidad Pública de Navarra (UPNA), Spain, in 1999 and 2005, respectively. From February 1999 to April 2000, he was a Microwave Commissioning Engineer with Siemens/Italtel, deploying microwave access systems. From May 2000 to December 2008, he was a Radio Access Engineer with Telefónica Móviles, performing radio network planning and optimization tasks in mobile network deployment. He was an Assistant Lecturer with the Electrical and Electronic Engineering Department, UPNA, from February 2003 to May 2009. From January 2009 to May 2009, he was a Co-Founding Member, the Director of Tafco Metawireless, and a spin-off company with UPNA. In June 2009, he was an Associate Professor with the EE Department, and the Department Head, from January 2012 to July 2018. From January 2018 to May 2018, he was a Visiting Professor with the Kuwait College of Science and Technology, Kuwait. He has also been the Department Head, since July 2019. He is currently affiliated with the Institute for Smart Cities (ISC), UPNA, which hosts around 140 researchers. He is also the Head of the ICT Section. He has more than 500 contributions in indexed international journals, book chapters, and conference contributions. His research interests include computational electromagnetics applied to analysis of complex electromagnetic scenarios, with a focus on the analysis, design, and implementation of heterogeneous wireless networks to enable context aware environments. He received the CST 2003 and CST 2005 Best Paper Award, the Ph.D. Award from the Colegio Oficial de Ingenieros de Telecomunicación (COIT), in 2006, the Ph.D. Award UPNA, in 2010, the First Juan Gomez Peñalver Research Award from the Royal Academy of Engineering of Spain, in 2010, the XII Talgo Innovation Award, in 2012, the IEEE 2014 Best Paper Award, in 2014, the ECSA-3 Best Paper Award, in 2016, and the ECSA-4 Best Paper Award, in 2017.